Laser and Particle Beams (2010), *28*, 421–427.

doi:10.1017/S026303461000042X

An initial design of hohlraum driven by a shaped laser pulse

KE LAN, PEIJUN GU, GUOLI REN, XIN LI, CHANGSHU WU, WENYI HUO, DONGXIAN LAI, AND XIAN-TU HE

Institute of Applied Physics and Computational Mathematics, Beijing, People's Republic of China

(RECEIVED 24 March 2010; ACCEPTED 1 June 2010)

Abstract

In this paper, the plasma-filling model was extrapolated to the case of a hohlraum driven by a shaped laser pulse, and this extended model was used to obtain an initial design of the hohlraum size. A density criterion of $n_e = 0.1$ was used for designing hohlraums which have low plasma filling with maximum achievable radiation. The method was successfully used to design a half hohlraum size with a three-step laser pulse on SGIII prototype and a U hohlraum size with shaped laser pulse for ignition. It was shown that the extended model with the criterion can provide reasonable initial design of a hohlraum size for optimal designing with a two-dimensional code.

Keywords: Hohlraum design; Inertial fusion; Plasma filling

INTRODUCTION

Since the hohlraum target plays a key role in the study of indirect drive inertial fusion study, the experimental and theoretical target design, and simulation continuously attract extensive interests and efforts worldwide (Aleksandrova *et al.*, 2008; Atzeni & Meyer-Ter-vehn, 2004; Borisenko *et al.*, 2008; Bret & Deutsch, 2006; Chatain *et al.*, 2008; Deutsch *et al.*, 2008; Eliezer *et al.*, 2007; Foldes & Szatmari, 2008; Hoffmann, 2008; Holmlid *et al.*, 2009; Hora, 2007; Imasaki & Li, 2007; Koresheva *et al.*, 2009; Li *et al.*, 2010; Ramis *et al.*, 2008; Rodriguez *et al.*, 2008; Strangio *et al.*, 2009; Winterberg, 2008; Yang *et al.*, 2008). The optimal size of a hohlraum is a trade-off between the requirements for energy and power, and the need for symmetry and acceptable plasma filling. Hence, a series of theory for target study have been developed, such as the hohlraum coupling efficiency theory, capsule radiation uniformity theory (Lindl, 2004), and plasma-filling model (Schneider *et al.*, 2006). In order to design a suitable hohlraum driven by a given laser source, we often use a two-dimensional (2D) hydrodynamic code to select the optimum hohlraum size by simulation. However, what is the initial size of the hohlraum that we should put into 2D simulation for further optimization? As known, the optimization searching process may be extremely laborious and computationally expensive if without a suitable initial value. In this paper, we will present a method for giving a suitable initial hohlraum size by using an extrapolated plasma-filling model, which was developed under the condition of a constant input laser power (Schneider *et al.*, 2006). In the following text, we will first extend the plasma-filling model to the condition of shaped laser pulse. Second, with this extended model, we will give an initial size of a half Au hohlraums, which is driven by a three-step laser pulse on SGIII prototype laser facility. This half hohlraum is used to test the optical diagnostics VISAR on SGIII prototype, and a low plasma filling with maximum achievable radiation is required in the hohlraum. Third, we will use our 2D simulation code Laser with Atomic, Radiation and Electron hydroDynamic code for Hohlraum physics study (LARED-H) (Duan *et al.*, 2002; Pei, 2007) to search the optimal size of the half hohlraum by simulation. The initial half hohlraum size obtained from above extended model will be used as an initial input. As it will be shown, the optimum hohlraum size obtained by simulation is close to its initial design. In the fourth part, we further use the extended plasma-filling model to obtain an initial design of the U hohlraum under laser pulse for ignition. Finally, we will present a summary.

PLASMA-FILLING MODEL FOR THE HOHLRAUM DRIVEN BY A SHAPED PULSE

In this section, we first relate the radiation temperature T_r to input laser power P and time τ by power balance (Sigel *et al.*,

Address correspondence and reprint requests to: Xin Li, Institute of Applied Physics and Computational Mathematics, P.O. Box 8009-14, Beijing, 100088, People's Republic of China. E-mail: li_xin@iapcm.ac.cn

1988), and then extend the plasma-filling model (Dewald *et al.*, 2005; McDonald *et al.*, 2006; Schneider *et al.*, 2006) to the case of a hohlraum driven by a shaped laser pulse.

In a hohlraum driven by a laser pulse, the radiation temperature T_r in steady-state conditions is related to input laser power P *via* the power balance:

$$\eta P = \sigma T_r^4\{(1-\alpha)A_W + A_H\}, \tag{1}$$

where η is the laser-to-X-ray coupling efficiency, A_W is the hohlraum wall area, A_H is the hohlraum hole area, α is the albedo of wall, and σ is the Stefan-Boltzmann constant. Under a radiation that is proportional to time, the albedo at time τ can be expressed as:

$$\alpha = 1 - H/(T_r^{\gamma}\tau^{\beta}), \tag{2}$$

where H, γ, and β are parameters related to radiation temporal profile.

We can approximately relate T_r to P and τ from Eqs. (1) and (2) by defining a hohlraum geometrical factor:

$$f_H = 1 + \frac{A_H}{(1-\tilde{\alpha})A_W}, \tag{3}$$

in which $\tilde{\alpha}$ is an average albedo of wall over time. Inserting Eq. (3) into Eq. (1), we have:

$$\eta P \approx (1-\alpha)\, f_H A_W \sigma T_r^4. \tag{4}$$

Then inserting Eq. (2) into Eq. (4), we obtain:

$$T_r = DP^E\tau^F, \tag{5}$$

where

$$D \approx \left[\eta\left(Hf_H\sigma\, A_W\right)^{-1}\right]^{\frac{1}{4-\gamma}}, \tag{6}$$

$$E \approx \frac{1}{4-\gamma}, \tag{7}$$

$$F \approx \frac{\beta}{4-\gamma}. \tag{8}$$

If an appropriate $\tilde{\alpha}$ is given, then radiation temperature obtained in this way is very close to the accurate solution of Eqs. (1) and (2). When there is a capsule inside the hohlraum or there is a sample on the hohlraum wall, the hohlraum geometrical factor can be redefined by taking the area of capsule or sample into consideration.

In the plasma-filling model (Dewald *et al.*, 2005; McDonald *et al.*, 2006; Schneider *et al.*, 2006), the laser beam channel is characterized by laser power, electron density n_e, electron temperature T_e, and ionization state Z_h of the hot plasma inside laser channel. The radiation ablated volume surrounding the laser channel is characterized by the radiation temperature T_r and electron density Zn_i, in which Z is the ionization state and n_i is the ion density of the radiation volume. Note that all densities are expressed in unit of the critical density. It is assumed that the laser power per unit length absorbed *via* inverse bremsstrahlung in the laser hot channel equals to the power per unit length conducted out of the channel by thermal conduction. The filling time for the hot laser channel to reach density n_e can be obtained by the pressure balance equation for the laser channel and the surrounding plasma, and the equations relating Z_h to T_e and Z to T_r.

Now we extend this plasma-filling model to a case in which a hohlraum is driven by a shaped laser pulse with high contrasts (>1) between different steps. This condition is widely used in inertial fusion research to produce a time-dependent radiation to assure a nearly isentropic compression of capsule inside the hohlraum and achieve thermonuclear ignition. The maximum radiation temperature in the hohlraum is produced in the last step of laser pulse. We focus on the Au hohlraum here and assume that the differences of T_r between steps are large and the mass of wall material ablated in each step of radiation is much larger than that in its former step. Neglecting the influence of former radiation steps on ablation, the mass of wall ablated in each step can be calculated independently. However, in each step the wall albedo increases and contributes to the sum of the ablated mass, which eventually influences the plasma-filling time in the hohlraum.

Assuming that the laser pulse has J steps, we use P_j to denote the incident laser power, τ_j is the time width, $T_{r,j}$ is the radiation temperature, $T_{r,j} \propto (t - \sum_{j'=1}^{j-1}\tau_{j'})^{k_j}$, and α_j is the albedo of the jth step ($j = 1, \ldots, J$). The coupling efficiency from laser to X-ray is assumed to be the same for each step, and then Eqs. (1) and (2) for the jth step become:

$$\eta P_j = \sigma {T_{r,j}}^4\{(1-\alpha_j)A_W + A_H\}, \tag{9}$$

$$\alpha_j = 1 - H_j/({T_{r,j}}^{\gamma_j}\tau^{\beta_j}). \tag{10}$$

The corresponding hohlraum geometrical factor is:

$$f_{H,j} = 1 + \frac{A_H}{(1-\tilde{\alpha}_j)A_W}, \tag{11}$$

where $\tilde{\alpha}_j$ is an average albedo of the jth step. Same as above, we have:

$$T_{r,j} = D_j P_j^{E_j}\tau_j^{F_j}, \tag{12}$$

https://doi.org/10.1017/S026303461000042X Published online by Cambridge University Press

in which

$$D_j = \eta\,(H_j f_{H,j}\sigma A_W)^{-1}, \tag{13}$$

$$E_j = \frac{1}{4-\gamma_j}, \tag{14}$$

$$F_j = \frac{\beta_j}{4-\gamma_j}. \tag{15}$$

The mass ablated in the jth step of radiation in Au can be expressed as (Lindl, 1995):

$$m_j(\mathrm{g/cm^2}) = 2.3\times10^{-7}(T_{r,j}/\mathrm{eV})^{1.86} \times (3.44k_j+1)^{-0.46}(\tau_j/ns)^{0.54+1.86k_j}. \tag{16}$$

Thus, the total ablated mass is $\sum_{j=1}^{J} m_j$. We therefore have the material density ρ and the ion density n_i in the hohlraum:

$$\rho = \frac{S_{abl}}{V_{hohl}}\times\sum_{j=1}^{J} m_j, \tag{17}$$

$$n_i = 1.07\times10^3\times\frac{\lambda_L^2}{A}\times\frac{S_{abl}}{V_{hohl}}\sum_{j=1}^{J} m_j, \tag{18}$$

where S_{abl} ($\mathrm{cm^2}$) is the effective area of wall being ablated, V_{hohl}($\mathrm{cm^3}$) is the hohlraum volume, and A is the atomic mass of the hohlraum material. Considering hydrodynamic losses and coronal radiative losses from the laser beam entrance hole of the hohlraum, we take $S_{abl} = S_{hohl} - S_{LEH}$, where S_{hohl} is the inner area of the hohlraum, and S_{LEH} is the area of the laser entrance hole (LEH). For an Au hohlraum driven by a 3ω shaped laser pulse, we have

$$n_i = 0.67\times\frac{S_{abl}}{V_{hohl}}\sum_{j=1}^{J} m_j. \tag{19}$$

As we mentioned above, the maximum temperature in the hohlraum will be obtained in the last step of laser pulse, i.e., $T_{r,J} = D_J\,P_J^{E_J}\tau_J^{F_J}$. Hereafter, we neglect the index J for the last step. As in Schneider *et al.* (2006), considering the power balance between the laser power per unit length being absorbed *via* inverse bremsstrahlung in the laser hot channel, and that exiting the channel *via* thermal conduction, as well as the pressure balance between the laser channel and surrounding plasma, we obtain:

$$P(\mathrm{TW}) = 3.1\times10^{-16}\times n_i^{4.6}n_e^{-6.6}(T_r/eV)^{6.67}(1-n_e)^{0.5}. \tag{20}$$

Inserting $T_r = DP^E\tau^F$ into the above expression and solving for n_e, we obtain the average density in the last laser step:

$$n_e(1-n_e)^{-\frac{1}{13.2}} = 4.47\times10^{-3}\times D^{1.01}P^{1.01E-\frac{1}{6.6}}\tau^{1.01F}n_i^{0.697}. \tag{21}$$

Usually, $n_e << 1$ and $(1-n_e)^{-\frac{1}{13.2}} \sim 1$, so Eq. (21) can be rewritten as:

$$n_e \approx 4.47\times10^{-3}\times D^{1.01}\times P^{1.01E-\frac{1}{6.6}}\,\tau^{1.01F}n_i^{0.697}. \tag{22}$$

Furthermore, we can obtain the average electron temperature T_e in laser hot channel by using the pressure balance 1000 n_eT_e (keV) = ZnT_r (eV) and the scaling $Z = 3.15T_r^{0.45}$ (Lindl, 1995):

$$T_e(\mathrm{keV}) = 3.15\times10^{-3}n_e^{-1}n_iT_r^{1.45}. \tag{23}$$

When the plasma filling becomes serious, the laser absorption region shifts far from the hohlraum wall, and more, the hydrodynamic loss and the thin coronal radiative loss from LEH increase rapidly. The density $n_e = 0.1$ is usually used as a threshold that prevents the laser from propagating into the hohlraum due to absorption. For the models concerned in this paper, we use $n_e = 0.1$ as a criterion for giving initial size of a hohlraum in which a low plasma filling with maximum achievable radiation is required. Note that this is different from that used in Dewald *et al.* (2005), in which $\lambda_{IB} = 0.7R_{\mathrm{LEH}}$ is taken as a criterion for a hot hohlraum. Here, R_{LEH} is the LEH radius and λ_{IB} is the inverse bremsstrahlung absorption length.

INITIAL DESIGN OF A HALF HOHLRAUM UNDER A SHAPED LASER PULSE ON SGIII PROTOTYPE

In this Section, we use the extended plasma filling model to give an initial design of size of a half hohlraum driven by a 6 kJ three-step laser pulse with 1:4:16 contrasts at 0.35 μm on SGIII prototype laser facility. As it is explained above, this half hohlraum is used to test the optical diagnostics VISAR on SGIII prototype. A low plasma filling with maximum achievable radiation is required in the hohlraum. Eight laser beams from 45° angle of incidence cone simultaneously irradiate the hohlraum from one side. The power profile of the laser beams are shown in Figure 1. The durations of the three steps are 1.5 ns, 1 ns, and 0.6 ns, respectively. The ratio of hohlraum length L to radius R is taken as 1.7, i.e., $L/R = 1.7$. The radius of LEH is required to be 350 μm, and the laser-to-X-ray coupling efficiency in half hohlraum is around 70% on SGIII prototype.

In order to use the extended plasma-filling model to design hohlraum size under a given laser drive, firstly we need to know the temporal profile of the radiation in hohlraum and the time-dependent albedo of the wall in order to obtain coefficients of k_j, H_j, γ_j, β_j, and $\tilde{\alpha}_j$ in Eqs. (10), (11), and (16).

From our simulation, for cases we concern, the radiation profile coefficient k_j is mainly decided by laser profile if the plasma filling is not serious. Meanwhile, the albedo profile coefficients, H_j, γ_j, and β_j, are mainly decided by k_j. The average albedo $\tilde{\alpha}_j$ is decided by maximum T_r in every step, but only sensitive to T_r in the first step when T_r is relatively low. Moreover, our study reveals that the radiation ablation behavior of the wall obtained from 2D simulation

https://doi.org/10.1017/S026303461000042X Published online by Cambridge University Press

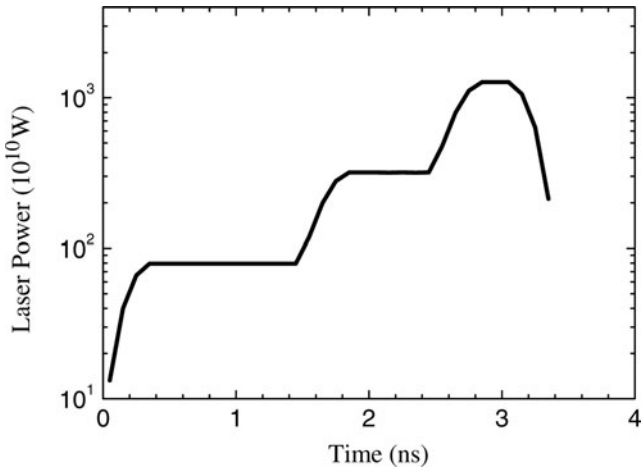

Fig. 1. Shaped laser pulse on SGIII prototype.

is very similar to that from one-dimensional simulation. The same result was also obtained in Suter *et al.* (1996).

Hence, we can first use our 2D code LARED-H to obtain a primary radiation in a half hohlraum with a reasonable supposed size under the given laser pulse, and then use one-dimensional code radiation hydrodynamic code of multi-groups (RDMG) (Feng *et al.*, 1999; Li *et al.*, 2010) to obtain the wall albedo under the radiation. Figure 2 shows the temporal T_r from LARED-H by taking R as 850 mm and L as 1450 mm, and the corresponding temporal albedo from RDMG.

Now, from the radiation and albedo obtained above, we can extract the coefficients by fitting: $k_j = 0.19$, 0.13, 0.12, $H_j = 8.5$, 7, 6.27, $\gamma_j = 0.66$, 0.66, 0.66, $\beta_j = 0.54$, 0.35, 0.54, for $j = 1$, 2, and 3, respectively. In addition, we take the average albedo of the three steps as: $\tilde{\alpha}_1 = 0.6$, $\tilde{\alpha}_2 = 0.7$, $\tilde{\alpha}_3 = 0.75$.

Inserting the above coefficients into Eqs. (12) and (20), we obtain the variations of n_e and T_r as R, as shown in Figure 3.

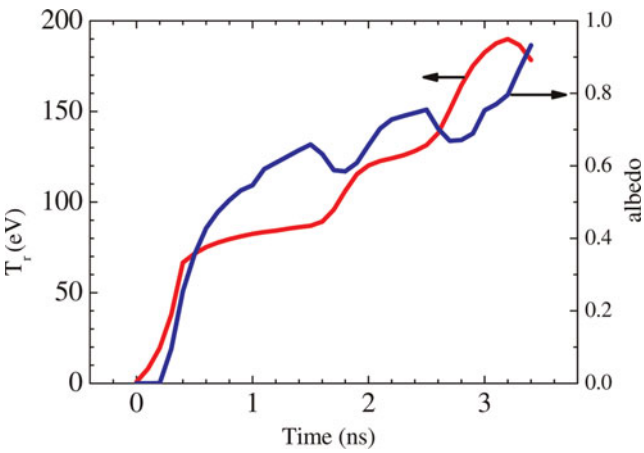

Fig. 2. (Color online) Temporal T_r (red line) in Au hohlraum from LARED-H and albedo (blue line) from RDMG. The hohlraum size is taken as $R = 850$ μm and $L = 1450$ μm.

Here, η is taken as 70%. As it is indicated, both n_e and T_r increases as R decreases. It means that the radiation is stronger and plasma filling is more serious in a smaller hohlraum. Thus, the criterion $n_e = 0.1$ gives the initial design of the half hohlraum as $R = 690$ μm with $T_r = 210$ eV.

2D SIMULATION RESULTS BY LARED-H

In the last Section, we obtained $R = 690$ μm as the initial design of the half hohlraum by using the extended plasma filling model. In order to find out an optimum design of the hohlraum size, we now use LARED-H to simulate three models of hohlraum with radii that are close to the initial design: $R = 600$, 650, and 700 μm. A total of 6 kJ of laser energy entered the half hohlraum from its LEH, and 10% laser energy is deducted after 2 ns due to laser plasma interaction loss from LEH.

In Figure 4, it shows spatial distribution of n_e in the hohlraum at 3 ns for the three models. As shown, the region of $n_e \leq 0.1$ is very small in the hohlraum of $R = 600$ μm, while relatively large in $R = 700$ μm hohlraum. In Figure 5, it presents the decay of the laser power in laser beam center along its transferring direction in the hohlraum. As indicated, the laser power decays to 37% of its initial value when it transfers to half of the hohlraum radius for $R = 600$ μm model, decays to 56% for $R = 650$ μm, and 77% for $R = 700$ μm. It means that most part of the laser has been absorbed by plasmas when it reaches half of its way to the hohlraum wall for $R = 600$ μm model, and hence it is not our optimum model. In Figure 6, it gives T_r in the hohlraum for the three models, obtained by post processing along the line about 30° from the hohlraum axis through LEH. As shown, the radiation temperature arrives, its maximum at around 3.2 ns, and it is about 233 eV, 221 eV, and 211 eV for the three models, respectively.

In order to get the maximum achievable radiation in a low plasma filling half hohlraum, the model of $R = 650$ μm is selected as the optimum design for the experiment. The

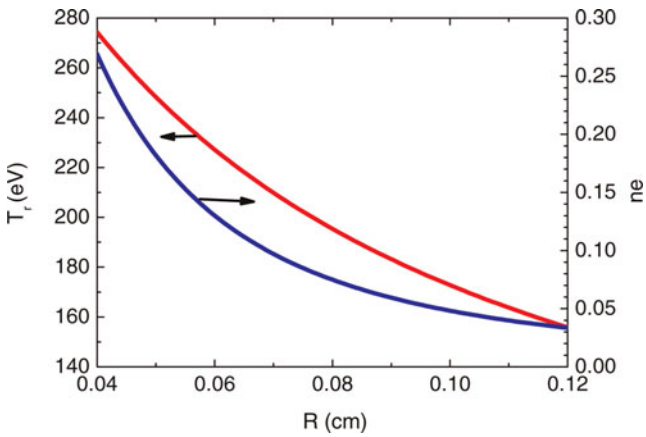

Fig. 3. (Color online) Variations of T_r (red line) and n_e (blue line) as R from Eqs. (12) and (20).

https://doi.org/10.1017/S026303461000042X Published online by Cambridge University Press

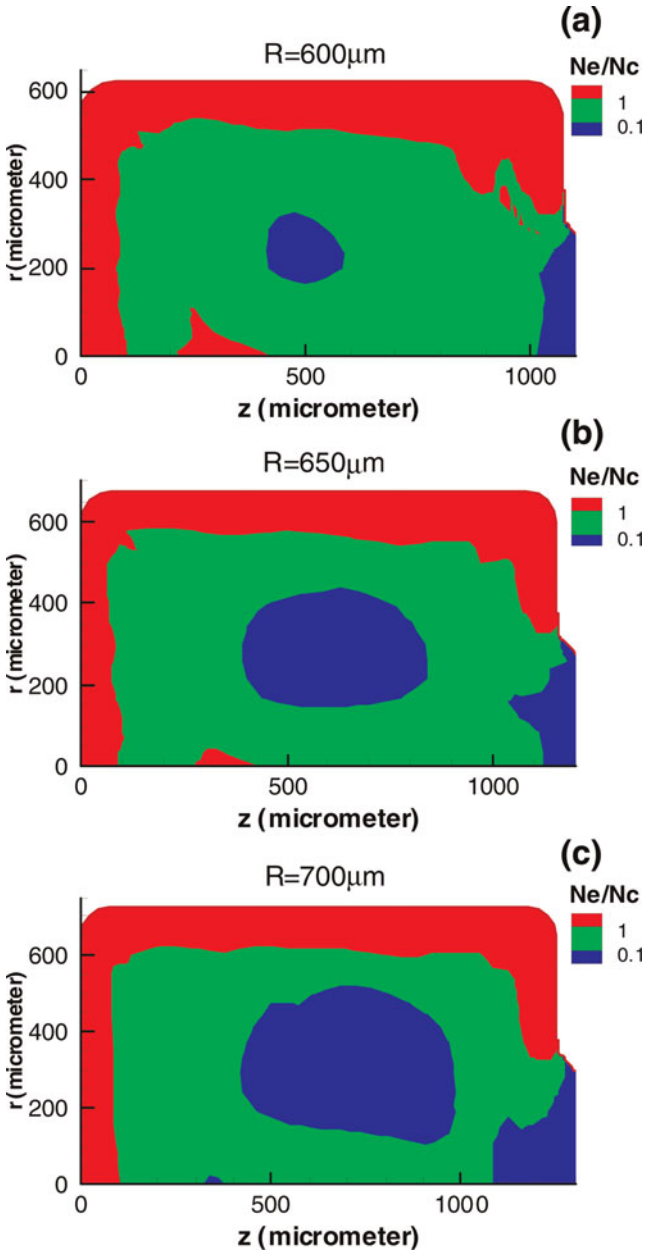

Fig. 4. (Color online) Spatial distribution of N_e/N_c in half hohlraum at 3 ns from LARED-H for the three models.

simulation results will be compared with the observations in a follow-up paper with experimental data we are collecting.

INITIAL DESIGN OF 300 eV IGNITION TARGETS OF NIF

In last section, we have used the extended plasma-filling model to obtain an initial design of a half hohlraum size to produce the maximum achievable radiation with low plasma filling under a given shaped laser pulse. In fact, the extended model can also be used to give an initial design of both the hohlraum size and the laser energy to produce a required radiation. Here, we use it to give an initial design

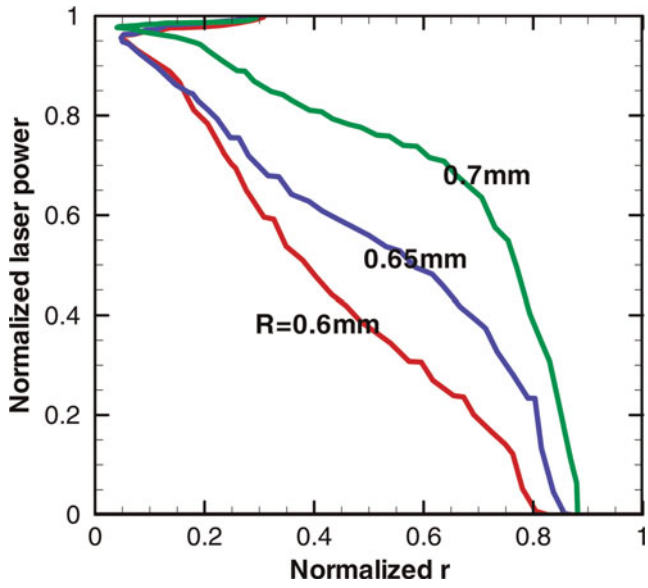

Fig. 5. (Color online) Decay of the laser power at 3 ns in laser beam center along its transferring direction in hohlraum for the three models. The abscissa is the radial position at the laser center and is normalized to hohlraum radius. The ordinate is the laser power at the laser center and is normalized to power at the center of LEH.

of the U hohlraum size and laser energy for producing the typical 300 eV ignition radiation designed for NIF (Hinkel *et al.*, 2008), although ignition hohlraum is filled with low-pressure gas while the plasma-filling model is made for an empty hohlraum. We take the contrasts between consecutive laser steps from Hinkel *et al.* (2008). The ratio of the hohlraum length to radius is taken as 3.62 and the coupling efficiency η is 75%.

In Figure 7, we present contour lines of $T_r = 300$ eV and $\eta_{e=0.1}$ in the plane of the hohlraum length and the laser energy for U hohlraum under the 300 eV ignition radiation drive. The intersection of $T_r = 300$ eV and $\eta_{e=0.1}$ gives the

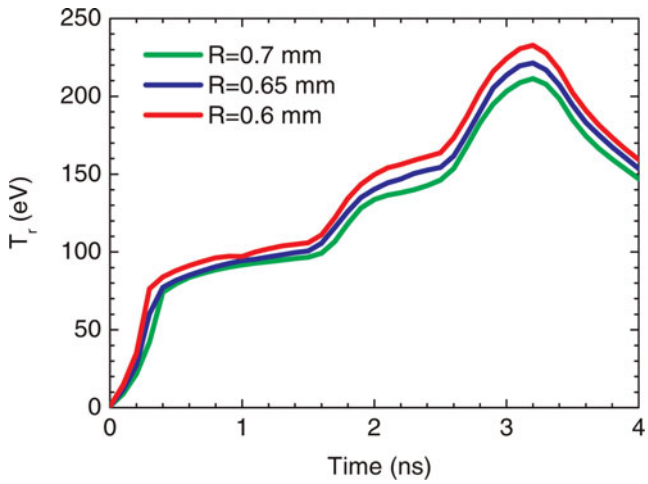

Fig. 6. (Color online) Postprocessed calculated T_r along the line about 30° from the hohlraum axis through LEH at 3 ns for the three models.

https://doi.org/10.1017/S026303461000042X Published online by Cambridge University Press

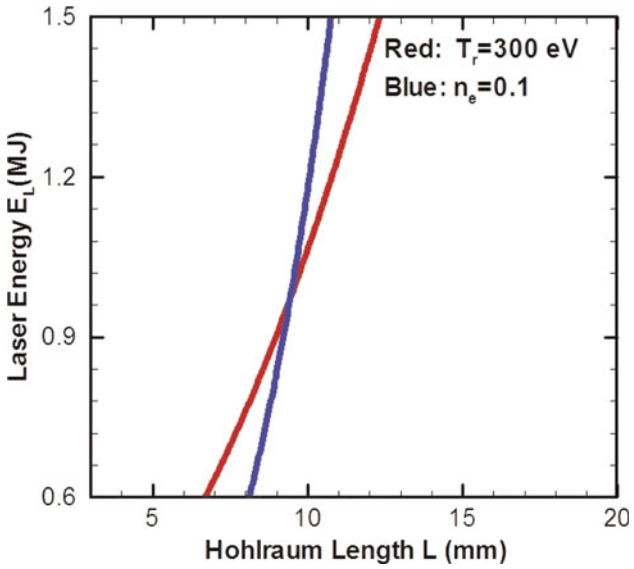

Fig. 7. (Color online) Contour lines of $T_r = 300$ eV (red line) and $n_e = 0.1$(blue line) in L/E_L plane for U hohlraum 300 eV ignition design.

initial design of 9.3 mm long hohlraum with 0.95 MJ laser energy, which is close to the 300 eV candidate hohlraum design for the 2009 ignition campaign on NIF (Hinkel *et al.*, 2008).

SUMMARY

In conclusion, the extended plasma-filling model can be used to give a reasonable initial design of the hohlraum size under a given laser pulse, or give a initial design of both the hohlraum size and laser energy to produce a required radiation. In particular, we can also have initial design of hohlraum with different geometries by this method, such as rugby-ball shaped hohlraum (Vandenboomgaerde *et al.*, 2007).

ACKNOWLEDGMENT

This work was performed under National Basic Research Program of China (973 program, No. 2007CB814800).

REFERENCES

Aleksandrova, I.V., Belolipeskiy, A.A., Koresheva, E.R. & Tolokonnikov, S.M. (2008). Survivability of fuel lasers with a different structure under conditions of the environmental effects: Physical concepts and modeling results. *Laser Part. Beams* **26**, 643–648.

Atzeni, S. & Meyer-Ter-Vehn, J. (2004). *The Physics of Inertial Fusion*. Oxford: Oxford Science Press.

Borisenko, N.G., Bugrov, A.E., Burdonskiy, I.N., Fasakhov, I.K., Gavrilov, V.V., Goltsov, A.Y., Gromov, A.I., Khalenkov, A.M., Kovalskii, N.G., Merkuliev, Y.A., Petryakov, V.M., Putilin, M.V., Yankovskii, G.M. & Zhuzhukalo, E.V. (2008). Physical processes in laser interaction with porous low-density materials. *Laser Part. Beams* **26**, 537–543.

Bret, A. & Deutsch, C. (2006). Density gradient effects on beam plasma linear instabilities for fast ignition scenario. *Laser Part. Beams* **24**, 269–273.

Chatain, D., Perin, J.P., Bonnay, P., Bouleau, E., Chichoux, M., Communal, D., Manzagol, J., Viargues, F., Brisset, D., Lamaison, V. & Paquignon, G. (2008). Cryogenic systems for inertial fusion energy. *Laser Part. Beams* **26**, 517–523.

Deutsch, C., Bret, A., Firpo, M.C., Gremillet, L., Lefebvre, E. & Lifschitz, A. (2008). Onset of coherent electromagnetic structures in the relativistic electron beam deuterium-tritium fuel interaction of fast ignition concern. *Laser Part. Beams* **26**, 157–165.

Dewald, E.L., Suter, L.J., Landen, O.L., Holder, J.P., Schein, J., Lee, F.D., Campbell, K.M., Weber, F.A., Pellinen, D.G., Schneider, M.B., Celeste, J.R., Mcdonald, J.W., Foster, J.M., Niemann, C.J. Mackinnon, A., Glenzer, S.H., Young, B.K., Haynam, C.A., Shaw, M.J., Turner, R.E., Froula, D., Kauffman, R.L., Thomas, B.R., Atherton, L.J., Bonanno, R.E., Dixit, S.N., Eder, D.C., Holtmeier, G., Kalantar, D.H., Koniges, A.E., Macgowan, B.J., Manes, K.R., Munro, D.H., Murray, J.R., Parham, T.G., Piston, K., Van Wonterghem, B.M., Wallace, R.J., Wegner, P.J., Whitman, P.K., Hammel, B.A. & Moses, E.I. (2005). Radiation-driven hydrodynamics of high-Z hohlraums on the national ignition facility. *Phys. Rev. Lett.* **95**, doi: 10.1103/PhysRevLett.95.215004.

Duan, Q., Chang, T., Zhang, W., Wang, G., Wang, C. & Zhu, S. (2002). Two-dimensional numerical simulation of laser irradiated gold disk targets. *Chinese J. Comp. Phys.* **19**, 57–61.

Eliezer, S., Murakami, M. & Val, J.M.M. (2007). Equation of state and optimum compression in inertial fusion energy. *Laser Part. Beams* **25**, 585–592.

Feng, T.G., Lai, D.X. & Xu, Y. (1999). An artificial-scattering iteration method for calculating multi-group radiation transfer problem. *Chinese J. Comput. Phys.* **16**, 199–205.

Foldes, I.B. & Szatmari, S. (2008). On the use of KrF lasers for fast ignition. *Laser Part. Beams* **26**, 575–582.

Hinkel, D.E., Callahan, D.A., Langdon, A.B., Langer, S.H., Still, C.H. & Williams, E.A. (2008). Analyses of laser-plasma interactions in National Ignition Facility ignition targets. *Phys. Plasmas* **15**, 056314.

Hoffmann, D.H.H. (2008). Intense laser and particle beams interaction physics toward inertial fusion. *Laser Part. Beams* **26**, 295–296.

Holmlid, L., Hora, H., Miley, G. & Yang, X. (2009). Ultrahigh-density deuterium of Rydberg matter clusters for inertial confinement fusion targets. *Laser Part. Beams* **27**, 529–532.

Hora, H. (2007). New aspects for fusion energy using inertial confinement. *Laser Part. Beams* **25**, 37–45.

Imasaki, K. & Li, D. (2007). An approach to hydrogen production by inertial fusion energy. *Laser Part. Beams* **25**, 99–105.

Koresheva, E.R., Aleksandrova, I.V., Koshelev, E.L., Nikitenko, A.I., Timasheva, T.P., Tolokonnikov, S.M., Belolipetskiy, A.A., Kapralov, V.G., Sergeev, V.T., Blazevic, A., Weyrich, K., Varentsov, D., Tahir, N.A., Udrea, S. & Hoffmann, D.H.H. (2009). A study on fabrication, manipulation and survival of cryogenic targets required for the experiments at the Facility for Antiproton and Ion Research: FAIR. *Laser Part. Beams* **27**, 255–272.

Li, X., Lan, K., Meng, X., He, X., Lai, D. & Feng, T. (2010). Study on Au + U + Au sandwich hohlraum wall for ignition targets. *Laser Part. Beams* **28**, doi:10.1017/S0263034609990590.

Lindl, J.D. (1995). Development of the indirect-drive approach to inertial confinement fusion and the target physics basis for ignition and gain. *Phys. Plasmas* **2**, 3933.

Lindl, J.D., Amendt, P., Berger, R.L., Glendinning, S.G., Glenzer, S.H., Haan, S.W., Kauffman, R.L., Landen, O.L. & Suter, L.J. (2004). The physics basis for ignition using indirect-drive targets on the National Ignition Facility. *Phys. Plasmas* **11**, 339–491.

Mcdonald, J.W., Suter, L.J., Landen, O.L., Foster, J.M., Celeste, J.R., Holder, J.P., Dewald, E.L., Schneider, M.B., Hinkel, D.E., Kauffman, R.L., Atherton, L.J., Bonanno, R.E., Dixit, S.N., Eder, D.C., Haynam, C.A., Kalantar, D.H., Koniges, A.E., Lee, F.D., Macgowan, B.J., Manes, K.R., Munro, D.H., Murray, J.R., Shaw, M.J., Stevenson, R.M., Parham, T.G., Van Wonterghem, B.M., Wallace, R.J., Wegner, P.J., Whitman, P.K., Young, B.K., Hammel, B.A. & Moses, E.I. (2006). Hard X-ray and hot electron environment in vacuum hohlraums at the National Ignition Facility. *Phys. Plasmas* **13**, doi: 10.1063/1.2186927.

Pei, W. (2007). The construction of simulation algorithms for laser fusion. *Commun. Comput. Phys*. **2**, 255–270.

Ramis, R., Ramirez, J. &Schurtz, G. (2008). Implosion symmetry of laser-irradiated cylindrical targets. *Laser Part. Beams* **26**, 113–126.

Rodriguez, R., Florido, R., Gll, J.M., Rubiano, J.G., Martel, P. & Minguez, E. (2008). RAPCAL code: A flexible package to compute radiative properties for optically thin and thick low and high-Z plasmas in a wide range of density and temperature. *Laser Part. Beams* **26**, 433–448.

Schneider, M.B., Hinkel, D.E., Landen, O.L., Froula, D.H., Heeter, R.F., Langdon, A.B., May, M.J., Mcdonald, J., Ross, J.S., Singh, M.S., Suter, L.J., Widmann, K. & Young, B.K. (2006). Plasma filling in reduced-scale hohlraums irradiated with multiple beam cones. *Phys. Plasmas* **13**, doi: 10.1063/1.2370697.

Sigel, R., Pakula, R., Sakabe, S. & Tsakiris, G.D. (1988). X-ray generation in a cavity heated by 1.3 or 0.44 mm laser light III Comparison of the experimental results with theoretical predictions for x-ray confinement. *Phys. Rev. A* **38**, 5779–5785.

Strangio, C., Caruso, A. & Aglione, M. (2009). Studies on possible alternative schemes based on two-laser driver for inertial fusion energy applications. *Laser Part. Beams* **27**, 303–309.

Suter, L.J., Kauffman, R.L., Darrow, C.B., Hauer, A.A., Kornblum, H., Landen, O.L., Orzechowski, T.J., Phillion, D.W., Porter, J.L., Powers, L.V., Richard, A., Rosen, M.D., Thiessen, A.R. & Wallace, R. (1996). Radiation drive in laser-heated hohlraums. *Phys. Plasmas* **3**, 2057.

Vandenboomgaerde, M., Bastian, J., Casner, A., Galmiche, D., Jadaud, J.-P., Laffite, S., Liberatore, S., Malinie, G. & Philippe, F. (2007). Prolate-spheroid ("rugby-shaped") hohlraum for inertial confinement fusion. *Phys. Rev. Lett*. **99**, doi: 10.1103/PhysRevLett.99.065004.

Winterberg, F. (2008). Lasers for inertial confinement fusion driven by high explosives. *Laser Part. Beams* **26**, 127–135.

Yang, H., Nagai, K., Nakai, N. & Norimatsu, T. (2008). Thin shell aerogel fabrication for FIREX-I targets using high viscosity (phloroglucinol carboxylic acid)/formaldehyde solution. *Laser Part. Beams* **26**, 449–453.